DEFORMATION AND FRACTURE PROPERTIES OF STEEL PIPE BEND WITH INTERNAL PRESSURE SUBJECTED TO IN-PLANE BENDING

Chitoshi MIKI[1], Takashi KOBAYASHI[2], Noritake OGUCHI[3], Takayoshi UCHIDA[4], Atsushi SUGANUMA[5] And Akihiko KATOH[6]

SUMMARY

In order to estimate the ultimate strength of steel pipe bend for gas transportation use, full-scale tests of both closing and opening mode bending were carried out. The final objectives of this research work is to optimize the allowable design strain or deformation of steel pipe bend subjected to permanent ground displacement induced by liquefaction due to a great earthquake. In order to discuss the allowable value, ultimate strength of steel pipe bends is studied with respect to crack initiation. Especially, the effects of materials, dimensions and geometry shape on ultimate strength of steel pipe bend were discussed by both experiments and numerical analysis.
It is confirmed that steel pipe bends largely deformed up to occurrence of a wrinkle before crack initiation. The ultimate strength of steel pipe bend was evaluated at least 30% as a local strain independent of materials. The dependency of ultimate bending angle on original center angle of pipe bend was clarified.

INTRODUCTION

In 1995, a great earthquake, Hyogoken-nambu earthquake occurred in western part of Japan. Not only many kinds of structures were damaged, but a lot of precious lives were lost. Since the earthquake, it began to revise seismic design codes for various structures in Japan..

Japan Gas Association started a research work on the safety of buried gas transportation pipeline subjected to permanent ground displacement due to a large earthquake. Especially, ultimate strength of steel pipe bend is one of the focus of this research work, because deformation of pipeline due to the ground motion would be concentrated to near bend parts of pipeline due to its flexibility. However, a few studies [1-3)] have been made on the ultimate strength of steel pipe bends. There has been several studies [4-8)] on the deformability of steel pipe bends subjected to in-plane bending, but in those studies, large deformation region beyond maximum moment point has not been investigated precisely. Furthermore, the effects of internal pressure on the ultimate strength of steel pipe bend has not been studied previously.

Therefore, many types of full-scale specimens were tested both under closing and opening mode of in-plane bending up to a occurrence of crack initiation or the limit of testing apparatus capacity. In most tests, internal pressure was applied to the bend specimen in order to clarify the ultimate strength of pipe bend under internally pressurized condition. And also, numerical simulations were performed to investigate the strain and stress distributions of those specimens subjected to bending.

As results, many important information such as the effect of internal pressure on the ultimate strength of steel pipe bend, ultimate strain or ultimate bending angle of steel pipe bend which indicates the initiation of crack were obtained.

This report describes outline of these research work and the ultimate strength of steel pipe bend subjected to in-plane bending.

[1] *Department of Civil Engineering, Tokyo Institute of Technology, Tokyo Japan. E-mail miki@cv.titech.ac.jp*
[2] *Tokyo Gas Corporation, Tokyo Japan. E-mail ktakashi@tokyo-gas.co.jp*
[3] *Tokyo Gas Corporation, Tokyo Japan. E-mail yuri_o@tokyo-gas.co.jp*
[4] *Osaka Gas Corporation, Osaka Japan. E-mail takayoshi-uchida@osakagas.co.jp*
[5] *Toho Gas Corporation ,Nagoya Japan. E-mail suganuma@tohogas.co.jp*
[6] *NKK Corporation, Kawasaki Japan. E-mail katoaki@lab.keihin.nkk.co.jp*

EXPERIMENTS

Tested Specimens

Full-scale specimens were used for bending tests. Table 1 shows dimensions of tested specimens. Figure 1 shows geometry shape of a specimen. The materials of tested steel pipe bend were API 5L X65, API 5L X52 and JIS PT370. Table 2 shows specified mechanical properties of tested pipes. Diameters of specimens were 165mm to 610mm, and diameter to thickness ratios were 23 to 60. Radii of tested pipe bends were 3 times and 1.5 times of pipe diameter.

In order to estimate the geometrical shape effects of pipe bend, original center angle of pipe bend is varied from 11.25 degree to 90 degree. API grade pipes were fabricated by UOE process and induction bending. JIS grade pipes were seamless pipe and bent by mandrel bending.

Table 1 Tested specimens

No.	Material	Outside diameter D , mm	Wall thickness t , mm	D / t	Center angle , deg.	Radius of pipe bend R , mm	Bending mode	Internal pressure MPa
1	X65	610.0	15.1	40	90	3DR	Closing	0
2	X65	610.0	15.1	40	90	3DR	Closing	8.9
3	X65	610.0	15.1	40	90	3DR	Opening	0
4	X65	610.0	15.1	40	90	3DR	Opening	8.9
5	X65	610.0	15.1	40	90	3DR	Closing	8.9
6	X65	610.0	15.1	40	22.5	3DR	Closing	8.9
7	X65	610.0	15.1	40	11.25	3DR	Closing	8.9
8	X65	610.0	15.1	40	22.5	3DR	Opening	8.9
9	X65	610.0	15.1	40	11.25	3DR	Opening	8.9
10	PT370	165.2	7.1	23	90	1.5DR	Closing	7.4
11	PT370	165.2	7.1	23	22.5	1.5DR	Closing	7.4
12	PT370	165.2	7.1	23	90	1.5DR	Opening	7.4
13	PT370	165.2	7.1	23	22.5	1.5DR	Opening	7.4
14	X65	610.0	15.1	40	45	3DR	Closing	8.9
15	X65	610.0	15.1	40	45	3DR	Opening	8.9
16	X52	610.0	10.3	59	90	1.5DR	Closing	4.9
17	X52	610.0	10.3	59	90	1.5DR	Opening	4.9
18	X52	406.4	7.9	51	90	1.5DR	Closing	5.6
19	X52	406.4	7.9	51	22.5	1.5DR	Opening	5.6
20	X52	406.4	7.9	51	90	1.5DR	Closing	5.6
21	X52	406.4	7.9	51	22.5	1.5DR	Opening	5.6

Table 2 Specified Mechanical Properties of Tested Steel Pipe Bend

Material	Yield Strength (MPa)	Tensile Strength (MPa)	Elongation (%)
API 5L X65	≥448	≥530	≥23.5
API 5L X52	≥358	≥455	≥26
JIS PT 370	≥215	≥370	≥28

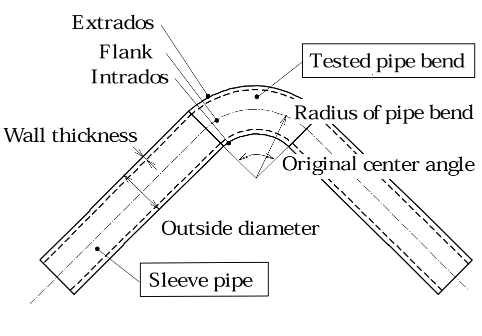

Fig.1 Geometry shape of a Specimen

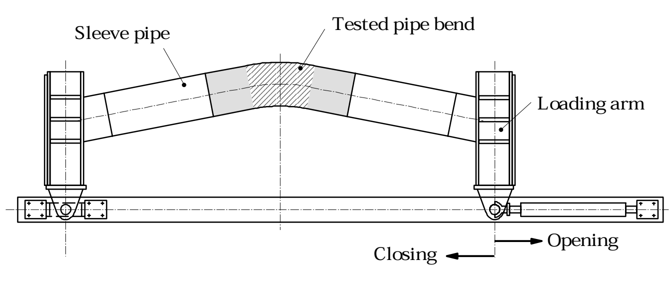

Fig. 2 Testing Apparatus for Bending Test

Test Procedure

Full-scale bending tests were carried out by using bending test apparatus shown in Fig.2.

Both closing mode and opening mode bending tests were carried out. For most specimens except No1. and No.2, internal pressure equivalent to hoop stress of 0.4 times SMYS (Specified Minimum Yield Strength) of a material was applied as shown in Table 1.

In closing mode bending, an end of a specimen was pulled inward, while in opening mode bending, an end was pushed outward direction. In closing mode bending, in order to conservatively evaluate ultimate strength, unloading process of both internal pressure and applied load was introduced. Because, in closing mode, a crack did not initiate even up to maximum displacement of capacity limit of loading apparatus under monotonic increase loading, but, when the unloading process of both applied load and internal pressure was introduced, a crack initiated at the unloading process.
In opening mode bending tests, cracks were initiated in monotonic increase process of applied bending angle. So, the unloading process was not taking account in opening mode bending tests. Figure 3 shows the schematic loading process of the tests for both closing and opening mode bending.
During a test, both of load and displacement at an end of specimens and strain distribution were monitored for all specimens. And to evaluate the macroscopic strain state, grid lines are drawn on the surface of the specimen and the distance of cross point of those grid lines were measured both before and after experiments.

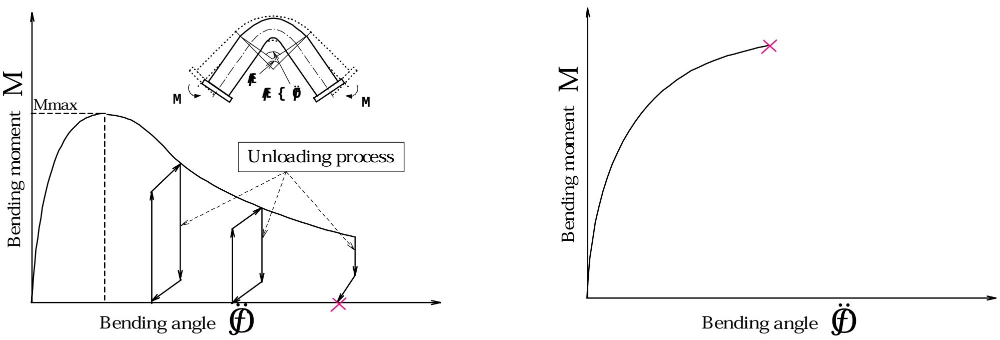

Fig. 3 Schematic loading process

Test results
Table 3 shows test results.
In table 3, ultimate state is defined as the initiation of crack. Photo 1. and 2. show the outlook of opening mode bending tests and closing mode bending test. It can be seen the ovalization of near central section due to bending.

Table 2 Test Results

No.	Material	Outside diameter D , mm	D / t	Center angle , deg.	Bending mode	Critical bending angle, deg.	Critical strain %	Remarks
1	X65	610.0	40	90	Closing	90	40	no crack
2	X65	610.0	40	90	Closing	90	>30	surface crack
3	X65	610.0	40	90	Opening	40	>30	thickness-through crack
4	X65	610.0	40	90	Opening	30	>30	thickness-through crack
5	X65	610.0	40	90	Closing	52	32	surface crack
6	X65	610.0	40	22.5	Closing	41	34	surface crack
7	X65	610.0	40	11.25	Closing	43	37	surface crack
8	X65	610.0	40	22.5	Opening	8.8	40	thickness-through crack
9	X65	610.0	40	11.25	Opening	7.6	36	thickness-through crack
10	PT370	165.2	23	90	Closing	>74	>29	no crack
11	PT370	165.2	23	22.5	Closing	77	58	surface crack
12	PT370	165.2	23	90	Opening	>81	>18	no crack
13	PT370	165.2	23	22.5	Opening	>79	>20	no crack
14	X65	610.0	40	45	Closing	43	34	surface crack
15	X65	610.0	40	45	Opening	16	36	thickness-through crack
16	X52	610.0	59	90	Closing	>79	>42	no crack
17	X52	610.0	59	90	Opening	52	33	thickness-through crack
18	X52	406.4	51	90	Closing	>71	>35	no crack
19	X52	406.4	51	90	Opening	56	31	thickness-through crack
20	X52	406.4	51	22.5	Closing	66	43	surface crack
21	X52	406.4	51	22.5	Opening	>71	>17	no crack

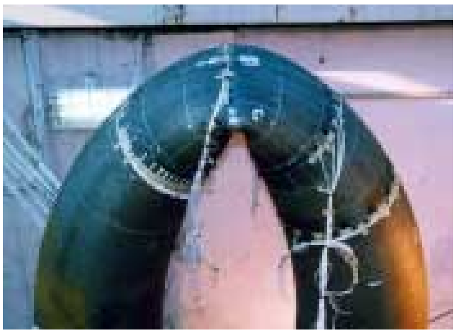

Photo 1 Closing mode bending

Photo 2 Opening Mode Bending

Figure 3 and 4 shows the relationship between bending moment and bending angle obtained in experiments.
In the case of closing mode bending, with the increase of bending angle, central section ovalized towards frank-frank direction, while in the case of opening bending mode, it ovalized towards intrados-extrados direction. It means that the stiffness of cross section decreases for closing mode bending, while, it increases for opening mode bending with the increase of applied bending angle.

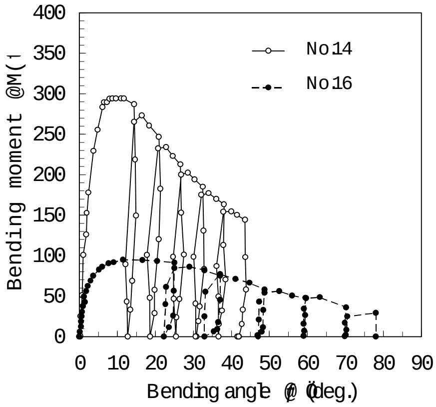

Fig. 3 Relation between Bending Moment and Bending Angle (Closing Mode)

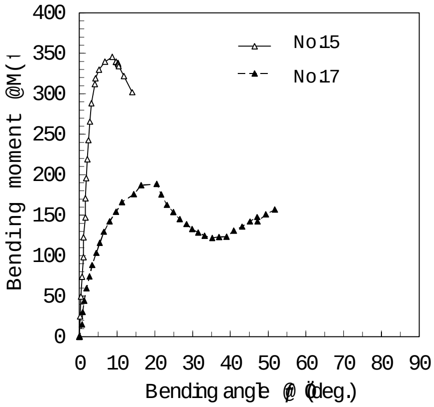

Fig.4 Relation between Bending Moment and Bending Angle (Opening Mode)

Final state of bending tests

As shown in Table 2, circumferential cracks initiated at near central section in closing mode bending tests, the cracks were not wall thickness- through cracks. Those cracks initiated at the process of unloading of internal pressure and applied load.
In opening mode bending tests, cracks initiated at opposite side where wrinkle had been observed. The wrinkle was observed at extrados side of near the end of bend part due to compression axial strain. With the increase of wrinkle deformation at extrados side, the axial tensile strain at intrados side remarkably increased.
Finally, cicumferential thickness-through crack initiated due to the axial tensile strain. Photo 3 shows a cut sample of tested pipe. It is observed steel pipe bends were largely deformed and wrinkled before a crack initiated.

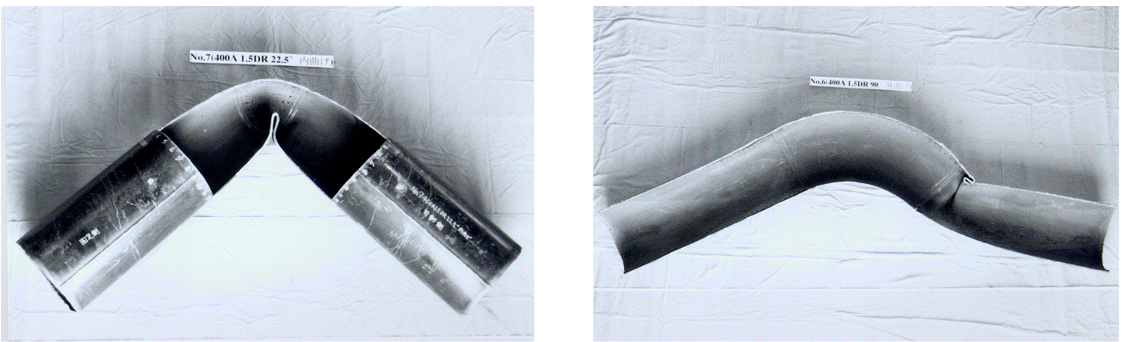

(a) Closing Mode Bending **(b) Opening Mode Bending**

Photo 3 A cut sample of tested pipe bend

3. NUMERICAL ANALYSIS

In order to estimate the deformation of pipe bend, numerical simulation by using elasto-plastic finite element analysis code ADINA were carried out. Table 3 shows the input conditions for the analysis. Four -node shell elements were used.

Table 3 Input conditions for numerical analysis

Code of calculation	ADINA Ver.6.1
Mesh	4-node shell element
Numerical model	1/4model (mirror symmetry) 1/2model (mirror symmetry)
Material property	elastic-plastic (Mises) Young's modulus E=206GPa Poisson's ratio =0.3 Yield strength$_y$=490532MPa Work-hardening ratio H_0'=2.1GPa
Geometrical B.C	constraint of node (sym , plane)
Mechanical B.C	described displacement

Figure 5 shows an examples of deformation and strain distribution of both closing and opening mode bending obtained by analysis.

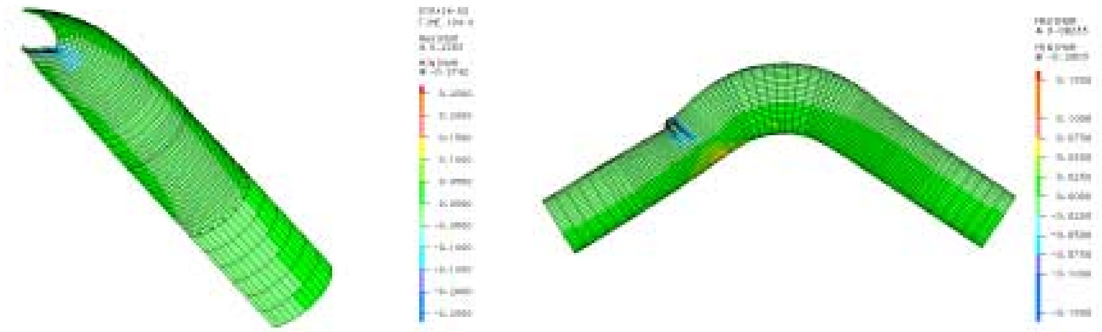

(a) Closing Mode Bending **(b) Opening Mode Bending**

Fig.5 Analytical results of deformation

Figure 6 shows the comparison of bending moment and applied bending angle relationship between experimental results and analysis. Both data agrees well.

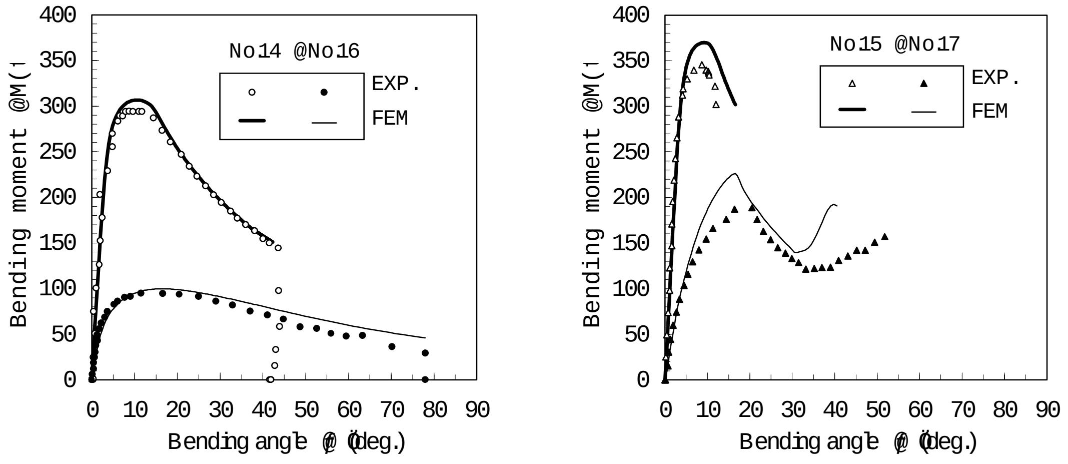

Fig.6 Comparison of bending angle and bending moment relationship between experiments and analysis

Figures 7 and 8 show the comparison of strain distribution at central section between experimental results and analysis. Except some peak values, both results agrees.

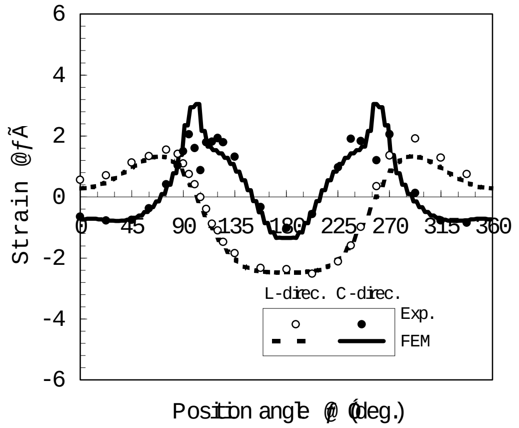

Fig.7 Strain Distribution at Central Section (Closing mode Bending)

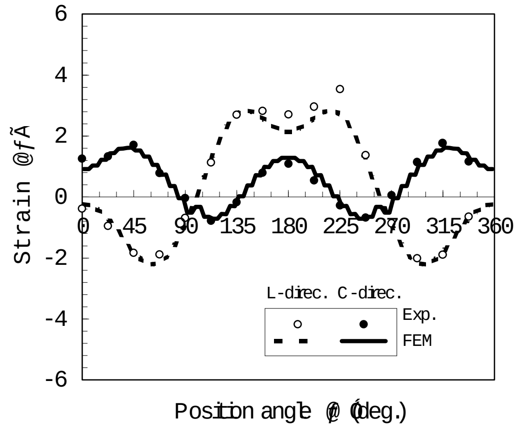

Fig.8 Strain Distribution at Central Section (Opening Mode Bending)

Figure 9 shows comparison of maximum strain between experimental results and analytical results for both closing mode and opening mode bending. In closing mode bending, both results agrees up to more than 20% of local strain, while, in opening mode bending, both data agrees within 10% of strains. Because, in opening mode bending, numerical analysis can not simulate the contact of wrinkled part as shown in Photo 3 (b).

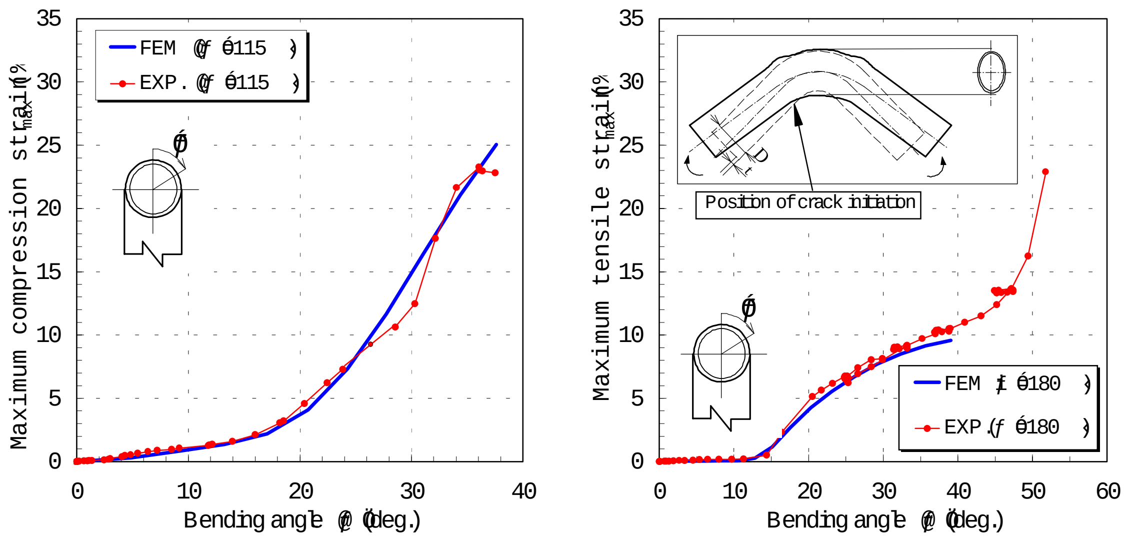

(a) Closing Mode Bending **(b) Opening Mode Bending**

Fig. 9 Comparison of Maximum Strain between Experiment and Analysis

DISCUSSIONS

Ultimate Strength of Steel Pipe Bend

If the effects of unloading process was taken account of, ultimate strain of steel pipe bends for various materials and pipe dimensions were obtained by full scale tests.

For closing mode bending, maximum strain occurs at central section of steel pipe bend, while for opening mode bending, maximum strain occurs at the vicinity of the end of bend part as shown in Fig.9.

In this study, ultimate strength of pipe bends was defined as the ultimate state in accordance with crack initiation. In the case of closing mode bending, in the vicinity of crack, large axial compressive strains had been accumulated until when the crack initiated. While, in opening mode bending, cracks initiated due to axial tensile strain. Therefore, above strains were recognized as critical values which indicates crack initiation of pipe bends subjected to in-plane bending.

Another candidate for critical values are applied bending angle at crack initiation, because it seems to be an index of deformability of pipe bends until crack initiated.

Considering experimental results shown in Table 3, the ultimate strain is estimated at least 30% for both closing and opening mode bending.

4.2 Effects of bend geometry shape on ultimate strength

The effects of original center angle of pipe bend on the ultimate strength is discussed. Figure 10 and 11 shows the relationship between ultimate values and original center angle of pipe bend for API 5L X65.

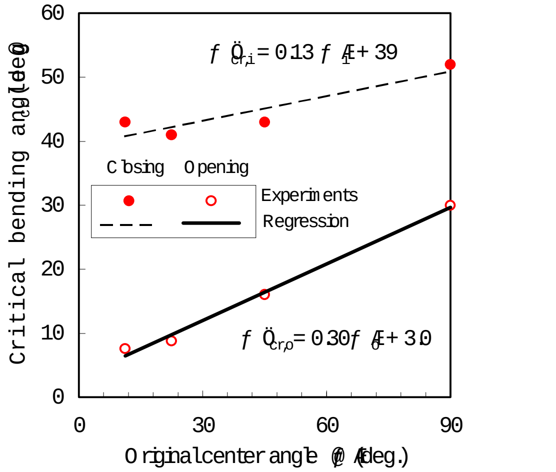

Fig.10 Relation between Ultimate Bending Angle and Original Center Angle of Pipe Bend for API X65

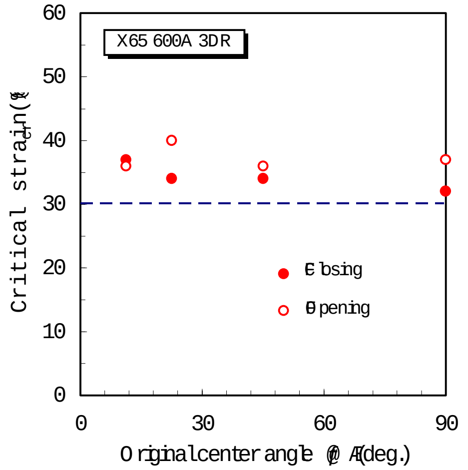

Fig.11 Relation between Ultimate Strain and Original Center Angle of Pipe Bend for API X65

The relationship between original center angle of a pipe bend and ultimate bending angle can be expressed as liner function as following equations for API 5L X65. The values of $\omega_{cr,i}$ and $\omega_{cr,o}$ are ultimate bending angle for closing mode and opening mode respectively.

$$\omega_{cr,I} = 0.13 \cdot \theta_i + 39$$

$$\omega_{cr,o} = 0.30 \cdot \theta_0 + 3.0$$

By this result, ultimate bending angle which indicate the crack initiation for API 5L X65 would be estimated for various initial center angle of bends.

As shown in Fig.11, critical strains are almost constant value of 30 to 40 % independent of original center angle of a pipe bend .

Effects of pipe material on the ultimate strength

Figure 12 shows the ultimate strain for various materials tested. Materials of steel pipe bends were API 5L X65, API 5L X52 and JIS PT370 in this study. The ultimate strain would be estimated at least almost 30% independent of materials.

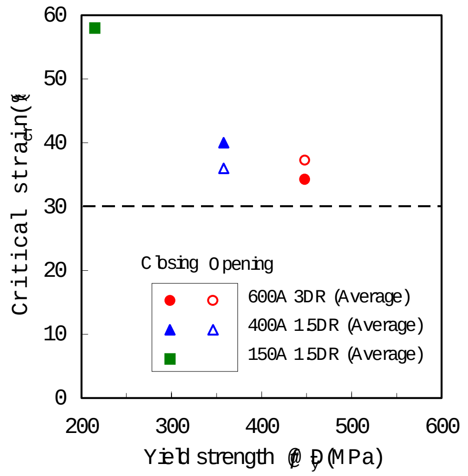

Fig.12 Ultimate strain for various pipe bend materials

CONCLUDING REMARKS

Both closing mode and opening mode bending tests for various steel pipe bend specimen were carried out. Furthermore, numerical simulations by using elasto- plastic finite element technique was also performed. Based on this study, following conclusions were obtained.

1) On the effects of internal pressure, the existence of internal pressure gives severe results which means lower ultimate strength for bending of steel pipe bend.
2) In the case of closing mode bending, crack initiated at unloading process, while, crack initiated at monotonic increase process of loading for opening mode bending.
3) If the ultimate strength is expressed in terms of local strain at vicinity of crack, it would be estimated 30% for both closing and opening mode bending.
4) The relation between ultimate bending angle and original center angle of pipe bend can be expressed following linear function.

$$\omega_{cr,I} = 0.13 \cdot \theta_i + 39$$

$$\omega_{cr,o} = 0.30 \cdot \theta_0 + 3.0$$

ACKNOWLEDGMENTS

After the 1995 Hyogoken Nanbu Earthquake, the Agency of Natural Resources and Energy, Ministry of International Trade and Industry entrusted the investigation of gas pipe behavior due to liquefaction to the Japan Gas Association. This investigation started in 1996 and will take five years to complete. It is supervised by the committee for investigation of the effect of liquefaction on gas pipelines, chaired by Dr. Tsuneo Katayama, the head of the National Research Institute for Earth Science and Disaster Prevention of the Science and Technology Agency. The authors express their gratitude to all persons concerned at MITI for their permission to publish this paper, and the committee members for their valuable suggestions.

REFERENCES:

1) Schmidt L.C., Lu J. P. and Morgan P.R., " The Influence on steel tubular strut load capacity of strain aging and Bauschinger effect." Journal of Construction Steel Research, Vol.14, No2 pp.107-119,1989
2) Suzuki N., "A study on the seismic design for buried pipeline taking account of permanent ground displacement" Doctor Thesis at Tohoku Univ., 1995
3) Y. Osawa and T.Nakano, " Low cycle fatigue strength of pipeline component. ", Piping and Plant Technology, Apr., 1983 (in Japanese)
4) Rodabaugh E. C. and George H.H., " Effect of Internal Pressure on Flexibility and Stress-Intensification Factors of Curved Pipe or Welding Elbows ", Trans. ASME, Vol.79, 1957
5) Y.Ono, N.Suzuki, A.Katoh and M.Yoshikawa, " The effects of internal pressure on the plastic defor4mation behavior of steel bend ", JSME No.96-10, Vol. B, 1996
6) Azzam T.J. and Scavuzzo R.J., " Analysis of Ratcheting in Pressurized Pipe Elbows ", ASME PVP-Vol.220, Seismic Engineering, 1991
7) Diem H., Blind D., Roos E., Wachter O. and Tolksdorf E. " Failure Behavior of thick-Walled Austenitic Pipe Bends under Cyclic Loading at Constant Internal Pressure. ", Nuclear Engineering and Design,151,1994
8) Scott P., Olson R. and Wilkowski G., " The IPIRG Pipe System Fracture Tests-Experimental Results." ASME PVP Vol.280, June 1994